Electron Beam Welding Studies of 25-mm-Thick Ti-6Al-4V Sections

A beam factor that can be used to compute penetration characteristics with various parameters is defined

BY G. THOMAS, V. RAMACHANDRA, K. V. NAGARAJAN, B. PANT, B. K. SARKAR AND R. VASUDEVAN

ABSTRACT. The effect of electron beam welding (EBW) parameters such as accelerating voltage, beam current and travel speed on depth of penetration for thick sections of Ti-6Al-4V alloy is detailed in this paper. Three distinct stages with different penetration characteristics have been identified. Based on the data collected, two factors, namely the beam factor (B_F) and the beam-diameter factor (BD_F) independent of travel speed have been evolved. Using B_F, a master curve has been generated for computing the depth of penetration. Computer analysis has also been carried out to develop mathematical equations for the variation of B_F with beam current for various accelerating voltages. The BD_F has been used to calculate the percentage change in beam diameter for various beam currents.

Introduction

The Ti-6Al-4V alloy is extensively used in aerospace applications owing to its high specific strength, good corrosion resistance to most of the fuels and oxidizers, ability to withstand high temperatures up to 500°C and good fabricability and weldability. The use of this alloy in India's Space Program is no exception. In its use as a launch vehicle component, a good weld is an important prerequisite. The two commonly used welding techniques for titanium alloys are the gas tungsten arc welding (GTAW) process with adequate inert gas shielding or an inert gas chamber and the electron beam welding (EBW) process. The EBW process is considered superior to others because of the obvious advantages (Refs. 1, 2) like a deep and narrow weld zone, reduced heat-affected zone (HAZ), ability to control gas content and high reliability. This method is used for welding (Refs. 3, 4) of both the high-pressure gas bottles and propellant storage tanks of the Indian Space Program. Obviously, variations in beam voltage, beam current and travel speed will have a pronounced effect on the geometry of the electron beam and the depth of penetration of the weld. Although achievements (Ref. 5) are reported on EB welding of sections up to 90-mm (3.5-in.) thick Ti-6Al-4V alloy, published data on weld parametric studies on thick sections of this alloy are limited. The earlier depth of penetration studies (Ref. 6) by the authors were limited to 6.5-mm (0.26-in.) thick plates. Therefore, a series of bead-on-plate welds were made on Ti-6Al-4V alloy for various combinations of voltage, current and travel speed. The effect of accelerating voltage, beam current and travel speed on depth of penetration is extensively dealt with in this paper.

KEY WORDS

Electron Beam Welding
Accelerating Voltage
Beam Current
Travel Speed
Depth Of Penetration
Power Density
Beam Factor
Beam Diameter Factor
Thermal Conduction
Thermal Perforation

Materials and Experimental Work

Material

The materials used in this parametric investigation were Ti-6Al-4V billets supplied by Timet, U.S.A. The billets were forged, cut and milled into pieces of 25 × 25 × 200 mm (1 × 1 × 7.9 in.) and were used for the bead-on-plate welds. The composition of the Ti-6Al-4V alloy is given in Table 1.

The experiments were done using a 12-kW-capacity, 150-kV Hawker Siddeley EBW machine.

Experimental Work

A series of bead-on-plate trials were made along the width of the piece at regular intervals. The pieces were given sufficient time before the welds for them to attain room temperature. The pieces containing the weld beads were cut at the center of the bead along the length. The cut surfaces were machined, polished and etched to view the fusion zone appearance. The depth of penetration and the width of the bead were also measured.

Parametric Study

The parameters generally used to describe the conditions in electron beam welding are the accelerating voltage, beam current, travel speed, beam diameter, work distance and beam focus. For a given focus and work distance, the beam diameter is largely influenced by the beam current and accelerating voltage. Hence, the important parameters that have pronounced effects on the penetra-

G. THOMAS, V. RAMACHANDRA, K. V. NAGARAJAN, B. PANT and B. K. SARKAR are with the Materials and Metallurgy Group, Vikram Sarabhai Space Center, Trivandrum, India. R. VASUDEVAN is a Professor, Department of Metallurgy, Indian Institute of Technology, Madras, India.

Table 1—Chemical Composition of Ti-6Al-4V

Element	Al	V	Fe	C	O	N	H	Ti
Weight %	6.14	3.97	0.12	0.032	0.0826	0.047	0.0028	Balance

tion capability of the beam are accelerating voltage, beam current and travel speed. In this study, the beam was always traversed on the workpiece, kept at a work distance of 190 mm (7.5 in.) and the beam focused 25 mm (1 in.) below the work surface. The bead-on-plate welds were made at constant accelerating voltages of 100, 110, 120, 130, 140 and 150 kV by varying the beam currents 10, 20, 30, 40, 50, 60 and 70 mA for various travel speeds of 150, 175, 200, 225, 250, 275 and 300 cm/min (59, 69, 79, 89, 98 and 118 in./min).

Results and Discussions

Beam Current

The effects of beam current on depth of penetration for various constant accelerating voltages and travel speeds are given in Fig. 1. The curves in the figure depict three distinct stages with three different slopes in decreasing order. A similar trend has been observed in titanium (KS-40) in the electron beam welding studies of Kiyoshi-Terai, *et al.* (Ref. 7), for various materials.

Stage 1

For accelerating voltages of 100 to 140 kV, Stage 1 extends up to a beam current of 20 mA only. The depth of penetration in this stage is limited to a few millimeters, as the beam power is relatively low. However, a small change in the beam current can bring about a large increase in depth of penetration as evidenced by the high slopes of this region. This is probably due to very low sensitivity of the beam diameter with respect to low beam currents and high accelerating voltages involved. Hence, the increase in beam currents in this region is completely reflected in the increase of power density, which in turn increases the depth of penetration. The penetration capability of this stage increases with the increase in accelerating voltages—Fig. 1. However, this decreases with an increase in travel speed. It is found that at higher accelerating voltages (150 kV), Stage 1 merges with Stage 2. Because of the relatively low beam power, the mechanism of beam penetration operating in this stage is predominantly by conduction, as seen in Fig. 2A, which shows a hemispherical shape for the weld.

Stage 2

Stage 2 covers the largest portion of the curve and EBW becomes most effective in this region—Fig. 3. This region gives a V-shaped geometry to the weld, as shown in Fig. 2B. The high beam power density of the stage is sufficient to cause evaporation of the metal under the beam, and this results in deep narrow

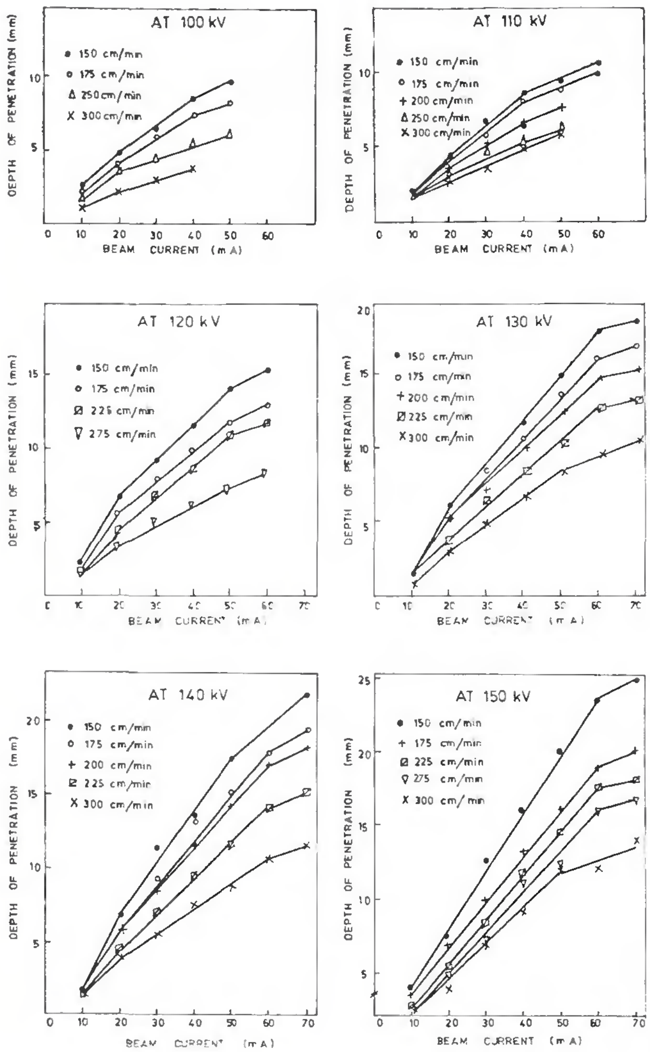

Fig. 1—Relationship between depth of penetration and beam current for various travel speeds

welds, and as the beam moves, the molten metal fills the vaporized hole and solidifies. As seen in Fig. 1, Stage 2 extends up to 60 mA for voltages of 150, 140 and 130 kV, up to 50 mA for 120 kV and up to 40 mA for 100 and 110 kV. Thus, we see the critical beam current at which Stage 2 ends decreasing with accelerating voltage. As in Stage 1, the penetration capability of the beam increases with accelerating voltage and low travel speeds. It is also seen that the penetration gain per unit increment in beam current is less during Stage 2 when compared to Stage 1. This is probably due to a significant beam diameter increase occurring in this stage that causes overall reduction in power density. This is not significant in Stage 1.

Stage 3

Stage 3 covers the last portion of the curve, and EBW becomes less effective in this region as depth-to-width ratio remains almost constant—Fig. 3. The penetrating capablity of the beam is much reduced in this region due to a reduction in power density resulting from a significant increase in beam diameter—Fig. 4.

Schwarz (Ref. 8) has derived a formula for beam diameter based on electron optics theory. The equation is

$$d = S\frac{L}{V}$$

where S is a constant depending on gun optics, L is beam current in mA, V is accelerating voltage in kV and d is beam diameter in 0.025 mm.

This equation indicates that the beam diameter is more at high currents and low voltages. Therefore, for any given voltage, there is a critical beam current above which the penetration capability appreciably reduces. Thus, we see in this region that any further increase in the beam current beyond the critical limit can hardly bring about any change in depth of penetration. As the beam diameter is large, the area of the metal under the beam is large, and hence much of the energy is spent in increasing the beam width rather than increasing the depth of penetration. The mechanism of penetra-

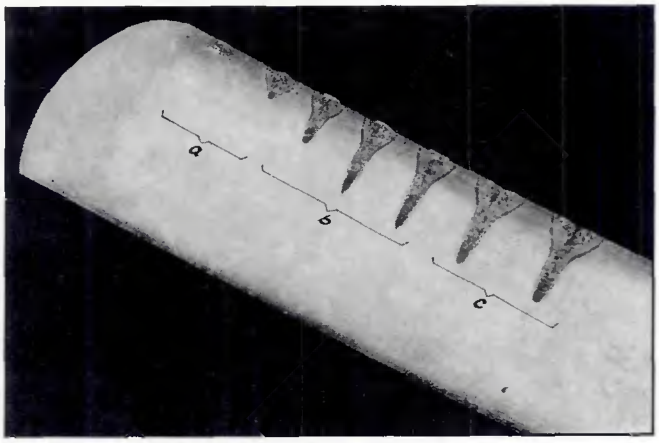

Fig. 2 — Shape of electron beam welds

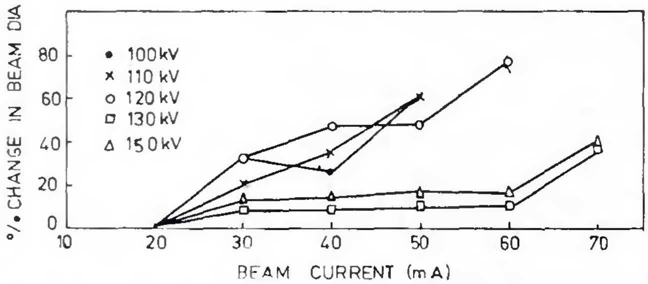

Fig. 4 — Variation of % change in beam diameter with beam current

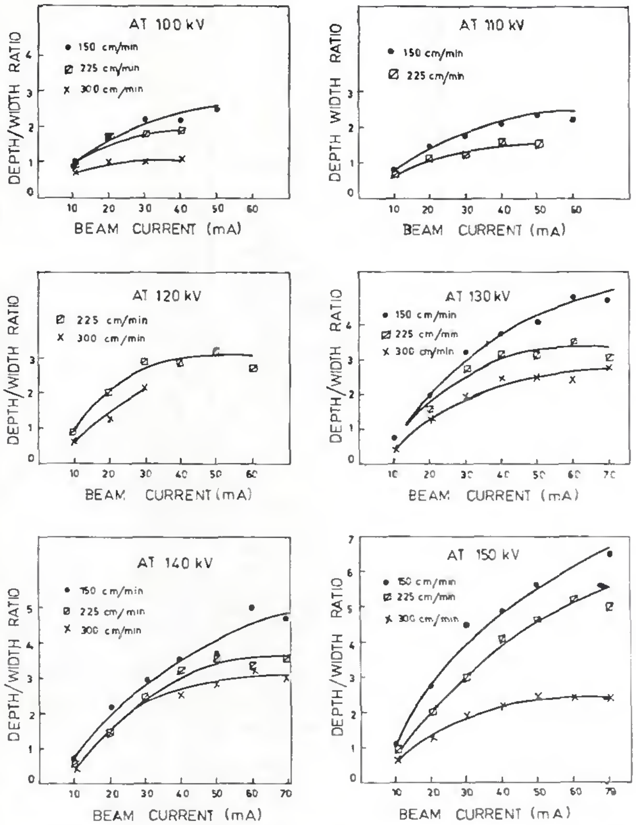

Fig. 3 — Relationship between depth-to-width ratio and beam current for various travel speeds

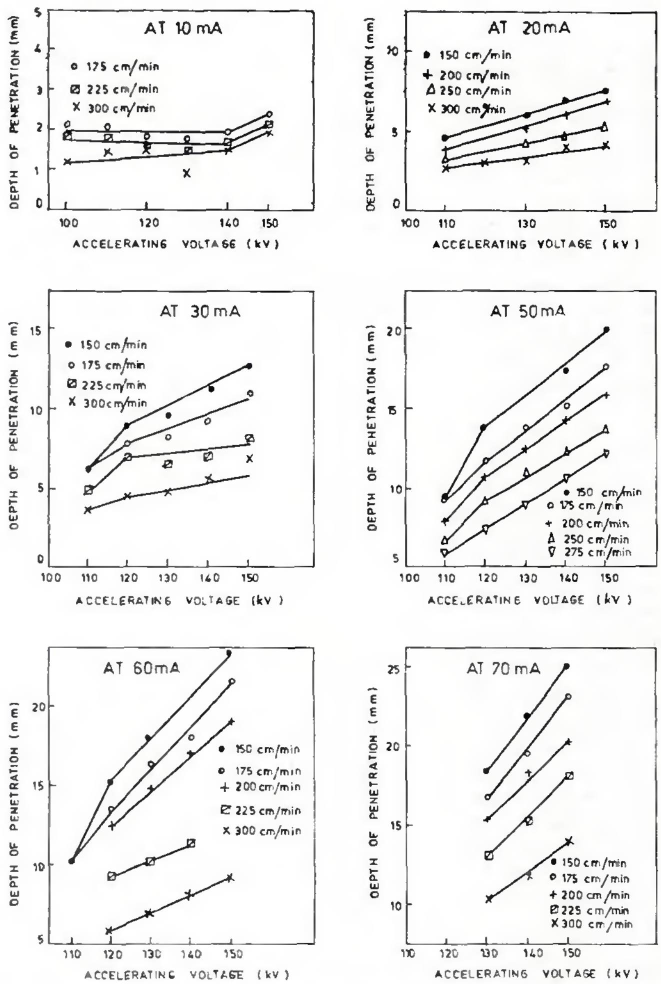

Fig. 5 — Relationship between depth of penetration and accelerating voltage for various travel speeds

tion prevalent in this stage is a combination of perforation and thermal conduction, as seen from the geometry of the weld in Fig. 2C.

Accelerating Voltage

The relationship between the depth of penetration and accelerating voltages for various beam currents and travel speeds is given in Fig. 5. It can be observed that the depth of penetration increases with accelerating voltage, and the slope of the curve tends to increase with beam current. This is also evident in the depth/width ratio plots with accelerating voltages for various beam currents and travel speeds shown in Fig. 6. In the case of beam currents of 60, 50 and 30 mA, a change in slope in the depth of penetration against an accelerating voltage curve is noticed at an accelerating voltage of 120 kV for all travel speeds. A similar effect has been reported by E. J. Konkol, *et al.* (Ref. 9), at an accelerating voltage of 125 kV during their studies on stainless steel. They have explained this on the basis of relativity effect imposed due to velocity of the electrons approaching that of light. Since the depth-of-penetration values are not available for accelerating voltages less than 130 kV and beam currents of 70 mA owing to machine limitations, it is not possible to say whether a similar effect would also be observed in this case. However, this change in slope is not noticed for beam currents of 10 and 20 mA. If the change in slope is attributed to the relativistic effect of electrons only, similar trends should have been indicated for these beam currents, also. A similar trend is not noticed in the EBW studies for various metals carried out by Kiyoshi-Terai, *et al.* (Ref. 7). It may also be mentioned that even at an accel-

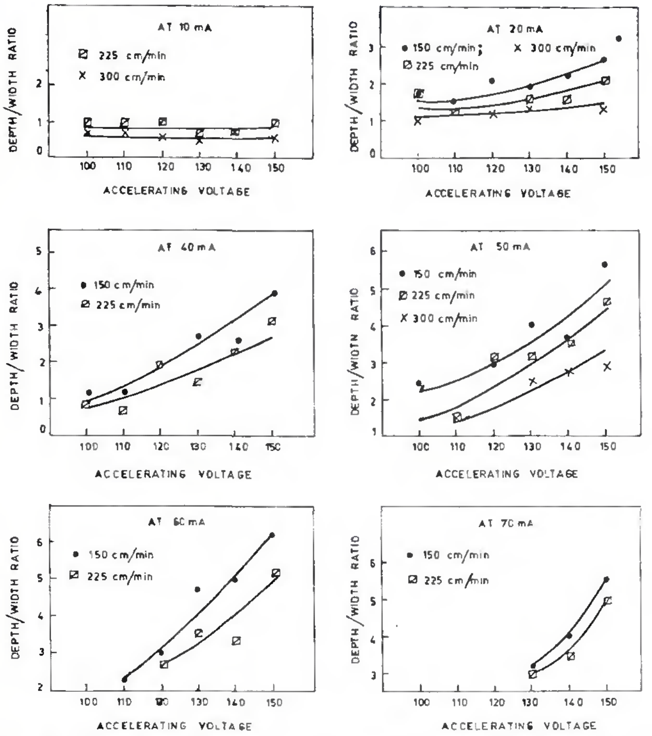

Fig. 6—Relationship between depth-to-width ratio and accelerating voltage for various travel speeds

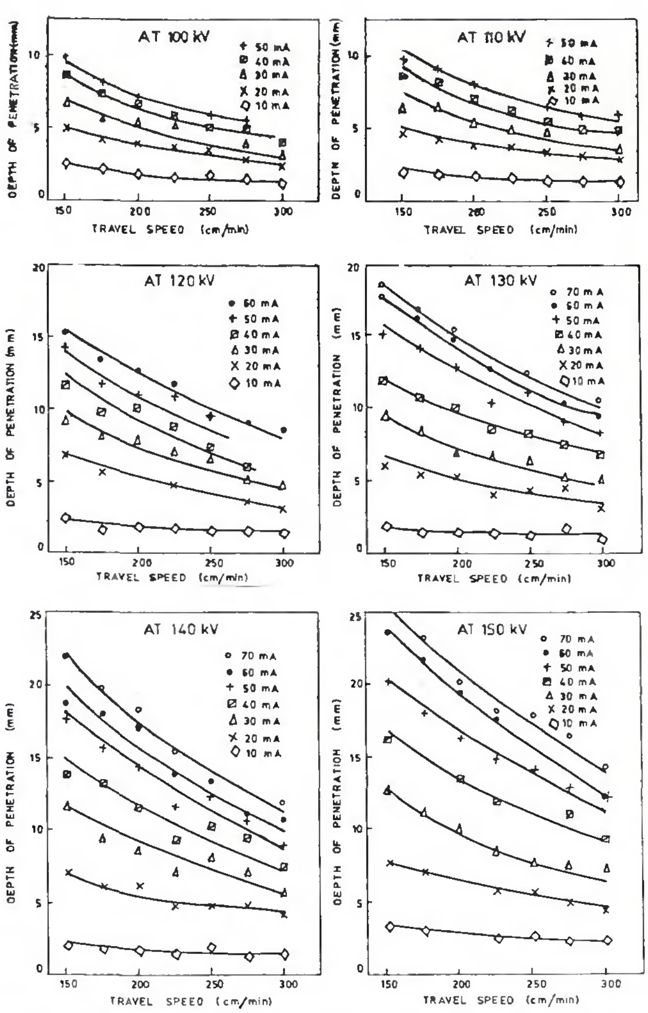

Fig. 7—Relationship between depth of penetration and travel speed for various beam currents

erating voltage of 150 kV, the velocity attained by electrons is only half that of light (Ref. 10). Thus, penetration constraints are caused not only by relativistic effect, but also by power density considerations. If the change in linearity at 120 kV was not found, variation in depth-to-width ratio with accelerating voltages shown in Fig. 6 should have been considerably larger.

Travel Speed

The varation in the depth of penetration with travel speed for various constant accelerating voltages and beam currents is shown in Fig. 7. The depth of penetration varies inversely with speed and the variation becomes more pronounced in the speed range of 150-250 cm/min. A similar effect is noticed in the case of depth/width ratio plots with travel speeds shown in Fig. 8. It is also noticed that the travel speed has a significant effect for high accelerating voltages and high beam currents.

Compared to accelerating voltage and beam current, travel speed has less effect on beam penetration since it does not directly contribute anything to beam power and only indirectly reduces the heat input/unit length of the weld.

Depth-to-Width Ratio

Depth-to-width ratio is an indication of the beam power density. The dependence of depth-to-width ratio on beam current for various constant accelerating voltages and travel speeds is shown in Fig. 3. It is evident from these curves that the variation in depth-to-width ratio is high for higher accelerating voltages and lower travel speeds. This ratio remains almost constant for higher beam currents. The influence of accelerating voltage on depth-to-width ratio for various constant beam currents and travel speeds is given in Fig. 6. These curves reveal that the depth-to-width ratio is high at higher beam currents and low travel speeds. The depth-to-width ratio is high at accelerating voltages beyond 130 kV. However, this is not found in the curve for 10 mA in Fig. 6 where the depth-to-width ratio remains almost constant for reasons already explained. The effect of travel speed on the depth-to-width ratio for various constant accelerating voltages and beam currents is given in Fig. 8. It is obvious from these curves that the depth-to-width ratio varies inversely with travel speed and it is negligible for travel speeds beyond 225 cm/min.

Beam Factor

The generalized dimensionless equation developed by Hablanian states that

$$b = C\frac{P}{TD}\sqrt{\frac{K}{Vd}} \qquad (1)$$

Where b = depth of penetration, c = proportionality constant, P = beam power, T = melting point, D = thermal diffusivity, V = welding speed, d = beam diameter and k = thermal conductivity. For a given material, the physical properties are constant. Hence Equation 1, can be written as

$$b = CPC_1\sqrt{\frac{1}{Vd}} \qquad (2)$$

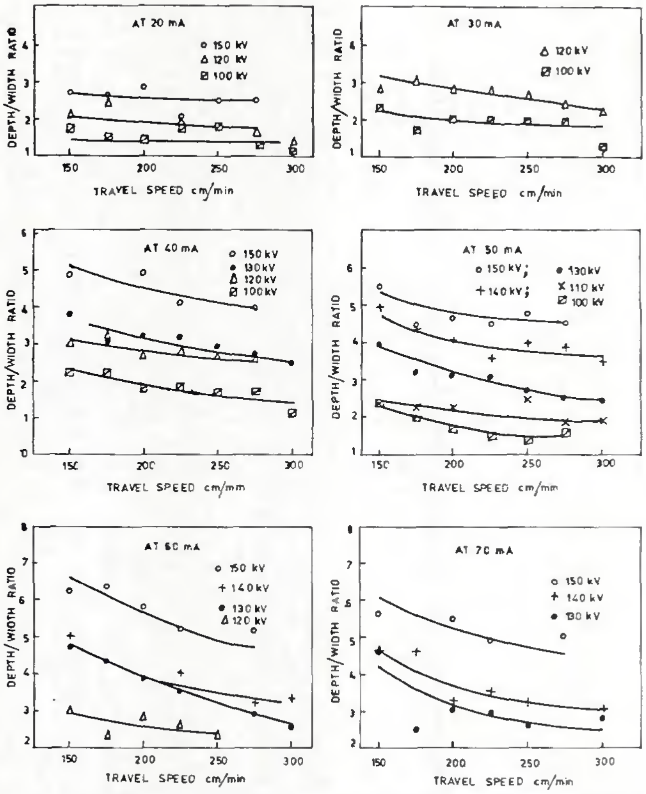

Fig. 8 — Relationship between depth-to-width ratio and travel speed for various accelerating voltages

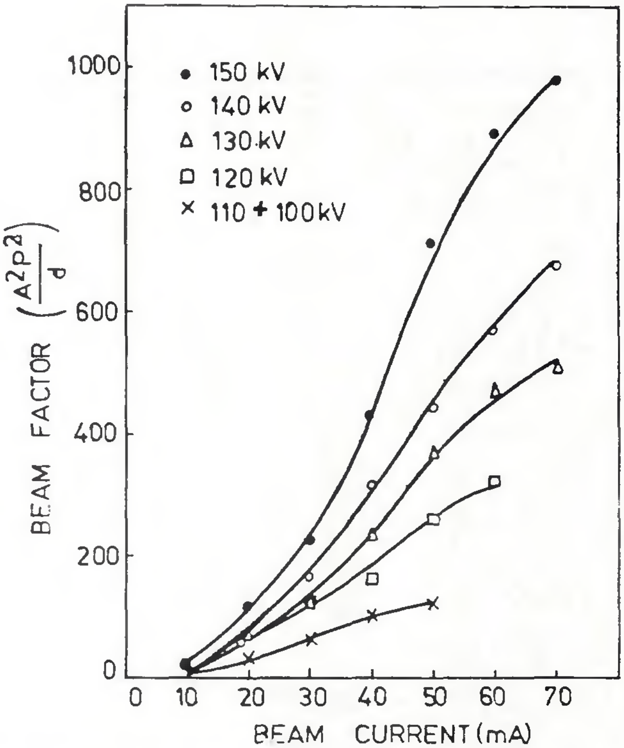

Fig. 9 — Relationship between beam factor and beam current

where $C_1 = \dfrac{\sqrt{K}}{TD}$

Equation 2 can be written as

$$b = A\frac{P}{\sqrt{Vd}} \tag{3}$$

where $A = CC_1$

$$b^2 = A^2\frac{P^2}{Vd} = \frac{B_F}{V}$$

where $B_F = \dfrac{A^2P^2}{d}$

$$2\ln b - \ln B_F = \ln V \tag{4}$$

From Equation 4, it is clear that the intercept of the linear curve 2 ln b versus ln V will give the term ln B_F. The term B_F is named as beam factor. The beam factors thus obtained are plotted against various beam currents, as shown in Fig. 9. Figure 9 thus evolved can be used as a master curve for determining the depth of penetration for any combination of accelerating voltages (100 to 150 kV), beam currents (10 to 70 mA) and travel speeds.

The beam factor multiplied by the inverse of the required travel speed V will give the square of the depth of penetration in mm^2. It is clear from Fig. 9 that the beam factor varies with beam current appreciably at higher accelerating voltages, and it remains almost the same for accelerating voltages of 100 and 110 kV.

The regression analysis carried out on the variation of B_F with beam current for various accelerating voltages has given the fifth-order polynomial for 100 and 110 kV and sixth-order polynomials for 120, 130, 140 and 150 kV, with regression coefficients varying from 0.998 to 1. The various constants of the polynomial are given in Table 2.

Percentage Change in Beam Diameter

The beam factor B_F has been used for determining the percentage change in beam diameter with beam current. The beam factor is

$$B_F = \frac{A^2P^2}{d} = \frac{A^2E^2I^2}{d}$$

where E = accelerating voltage and I = beam current. For a constant accelerating voltage, it is seen that the beam factor depends only on beam current and beam diameter. The effect of beam current can be eliminated from the beam factor by dividing it by I^2. The resulting term obtained is called the beam diame-

Table 2—Constants for the Polynomial Equation

$$(Y = A_0 + A_1X + A_2X^2 + A_3X^3 + A_4X^4 + A_5X^5 + A_6X^6)$$

	150 kV	140 kV	130 kV	120 kV	100 and 110 kV
A_0 =	265.267113415	799.813822519	13.840252029	136.181654775	10.8980425828
A_1 =	−80.3598442933	183.149538117	−5,6731966341	−31.0035133127	−4.74572115245
A_2 =	8.90371659072	−15.4987700599	1.35239127192	2.28248153981	0.65684688549
A_3 =	−0.431846280298	0.647149974051	$-7.96739124517 \times 10^{-2}$	−0.045785207877	$-2.78540448229 \times 10^{-2}$
A_4 =	$1.07550424951 \times 10^{-2}$	$-1.37265221699 \times 10^{-2}$	$2.28085687278 \times 10^{-3}$	$-4.0503434953 \times 10^{-4}$	$5.62142539112 \times 10^{-4}$
A_5 =	$-1.2836485673 \times 10^{-4}$	$1.44065088921 \times 10^{-4}$	$-2.92852711476 \times 10^{-5}$	$2.33856271614 \times 10^{-5}$	$-4.22900628932 \times 10^{-6}$
A_6 =	$5.80935058061 \times 10^{-7}$	$-5.94390250069 \times 10^{-7}$	$1.36642436705 \times 10^{-7}$	$-1.97670566853 \times 10^{-7}$	—

ter factor, B_D. The beam diameter factors B_{D_1} and B_{D_2} for beam currents I and I_2, respectively, can be written as

$$B_{D_1} = \frac{B}{d_1} \quad B_{D_2} = \frac{B}{d_2}$$

B is constant, and d_1 and d_2 are beam diameters at beam currents, I_1 and I_2.

$$\frac{B_{D_1} - B_{D_2}}{B_{D_2}} \times 100 = \frac{d_1 - d_2}{d_2} \times 100 \qquad (5)$$

Therefore, Equation 5 will give us the percentage change in beam diameter. Similarly, a beam diameter factor for constant beam current can also be arrived at.

The percentage change of beam diameter calculated with 20 mA as a reference for various beam currents at constant accelerating voltages is plotted for varying beam currents and shown in Fig. 4.

It is clear from Fig. 4 that the percentage change in beam diameter is maximum (60–80%) for lower accelerating voltages of 100, 110 and 120 kV, and minimum (25–40%) for accelerating voltages of 130, 140 and 150 kV. For all accelerating voltages, the percentage change in beam diameter becomes relatively high at high beam currents. For example, for accelerating voltages of 100, 110 and 120 kV the percentage change in beam diameter becomes appreciable after 40 mA, whereas for 130, and 150 kV, the change becomes appreciable only after 60 mA. These observations are in accordance with various stages seen in Fig. 1. Thus, a combination of high accelerating voltage and low beam current is ideal for achieving optimum depth of penetration.

Conclusions

1) Three distinctive stages with different penetration characteristics have been identified over varying beam currents at constant accelerating voltages and travel speeds.

2) The penetration mechanism operating for Stages 1 is presumed to be by thermal conduction, as contrasted to thermal perforation in Stage 2. In Stage 3, a combination of perforation and thermal conduction is operative.

3) For a constant accelerating voltage and travel speed, there exists a critical beam current, beyond which the depth of penetration does not increase appreciably, and the critical beam current reduces with the reduction of accelerating voltage.

4) The variation of the depth of penetration with beam current is more pronounced at lower travel speeds and higher accelerating voltages.

5) The variation of depth of penetration with accelerating voltage is high at high beam currents and remains almost negligible for a beam current of 10 mA.

6) The effect of travel speed on depth of penetration is appreciable in the speed range of 150 to 250 cm/min and becomes almost negligible between 250 to 300 cm/min.

7) The dependence of depth-to-width ratio on beam current for a given accelerating voltage and travel speed is appreciable for beam currents up to 50 mA and remains almost constant for 50 to 70 mA.

8) The variation of depth-to-width ratio with beam current is high for high accelerating voltages and low travel speeds.

9) A beam factor, B_F, and a beam diameter factor, B_D, independent of travel speed at constant accelerating voltages have been computed for various beam currents.

10) Using the beam factor, a master curve for computation of depth of penetration for any combination of accelerating voltages (100 – 150 kV), beam currents (10–70 mA) and travel speeds has been determined.

11) The beam factor varies appreciably with beam current for higher accelerating voltages and remains almost the same for 100 and 110 kV.

12) Polynomial equations of the fifth and sixth order have been developed for the variation of B_F with beam current for various accelerating voltages.

13) The percentage of change in beam diameter is large at lower accelerating voltages and high beam currents.

Acknowledgment

The authors wish to thank their colleages in alloy processing, fabrication, metallography and drafting sections of the Metallurgy and Ceramics Division (MAC) for the help and assistance rendered during the course of this work. The authors also express their deep sense of gratitude to Shri K. Murugesan, Special Materials Division, for carrying out the computer analysis and Shri D. Easwaradas, deputy director, Materials and Mechanical Systems, for his constant encouragement and guidance. The authors are also indebted to Dr. S. C. Gupta, director, Vikram Sarabhai Space Center for according his permission to publish this paper and also to the director of the Indian Institute of Technology, Madras, for the interest shown in this work. The authors are also grateful to GTRE, Bangalore, for carrying out the experimental work. The typing support rendered by Shri S. Sivaramakrishnan, MMG Office is gratefully acknowledged.

References

1. Paton, B. E. *et al.* 1976. Trends in the development of electron beam welding. *Automatic Welding* 29(10):57–62.
2. Russel, J. D. 1981. Development in heavy section EB welding. *Metal Construction* 13(10):49–52.
3. Ramachandra, V. *et al.* 1982. Development of Ti-6Al-4V gas bottle for satellite applications. *Trans. IIM* 35(2):127–135.
4. Ramachandra, V. *et al.* Development of titanium alloy reaction control system tanks and transition joints between Ti-6Al-4V and S.S.304 L for satellite control system. *Proceedings of the Symposium on Titanium Alloys for Aerospace and Chemical Applications*, Trivandrum, India. 1983.
5. Ryoichiro-Sasano, *et al.* Fundamental study on electron beam welding of heavy thickness 6Al-4V titanium alloy, Mitsubishi Heavy Industries Ltd., Japan.
6. Thomas, G. *et al.* 1982. Electon beam welding studies on 6.5-mm-thick Ti-6Al-4V plate. *Trans. IIM* 35(1):25–32.
7. Kioshi-Terai, *et al.* 1972. Effects of process parameter on the penetration depth in high-voltage electron beam welding. *Trans. Japan Welding Soc.* 3(1):12–23.
8. Schwarz, H. 1962. Electron beam processes at different voltages. *Trans. of 8th Vacuum Symposium*, Pergamon Press.
9. Konkol, P. J. *et al.* 1971. Parameter study of electron beam welding. *Welding Journal* 50(11):765-s to 776-s.
10. Meleka, A. K. 1971. *Electron Beam Welding, Principles and Parameters.* McGraw Hill.
11. Hablanian, M. H. 1962. A correlation of welding variables. *Proceedings of the Electron Beam Welding Symposium*, 5th Annual Meeting, Boston, Mass, p. 262.